Orbital Selective Commensurate Modulations of the Local Density of States in ScV_6Sn_6 Probed by Nuclear Spins

Robin Guehne[#], Jonathan Noky, Changjiang Yi, Chandra Shekhar, Maia G. Vergniory, Michael Baenitz and Claudia Felser

The two-dimensional kagome network have emerged as a key structural motif in modern solid state physics, because these networks host special electronic states related to Dirac cones, van Hove singularities, and flat bands, providing a rich playground for the study of critical phenomena including electronic correlation, superconductivity, and charge order. The V-based kagome metal ScV_6Sn_6 exhibits an unconventional charge density wave below approximately 96 K. To illuminate the interesting phenomena as well as the structural and electronic properties of ScV_6Sn_6 from a microscopic perspective, we employed ^{51}V nuclear magnetic resonance and density functional theory. The dynamics of the local magnetic field reflect the changes in the density of states of V, while the static local magnetic field reveals a substructure of Fermi level states, suggesting orbital-selective modulation of the local DOS.

This report documents a recently published work [1] resulting from a long-standing cooperation between the nuclear magnetic resonance (NMR) group of the Physics of Quantum Materials department and the Topological Quantum Chemistry department at the Max Planck Institute for Chemical Physics of Solids. While we initially investigated Weyl and Dirac semimetals (monopnictides TaP, TaAs, and NbP, as well as dipnictides like $TaSb_2$ [2, 3, 4, 5, 6, 7]), we later extended our focus to charge density wave (CDW) systems based on the kagome lattices.

In recent years, kagome networks – two-dimensional structures based on cornersharing triangles (Figure 1) – have attracted significant attention in the solid state physics community. The electronic band structure of kagome lattices features special dispersions, such as Dirac cones, saddle points associated with van Hove singularities, and flat bands. These dispersions are believed to play a central role for correlation effects, superconductivity, and charge order. Furthermore, kagome planes can be incorporated in a variety of chemical environments, providing the ability to chemically fine-tune a material to achieve well defined electronic properties.

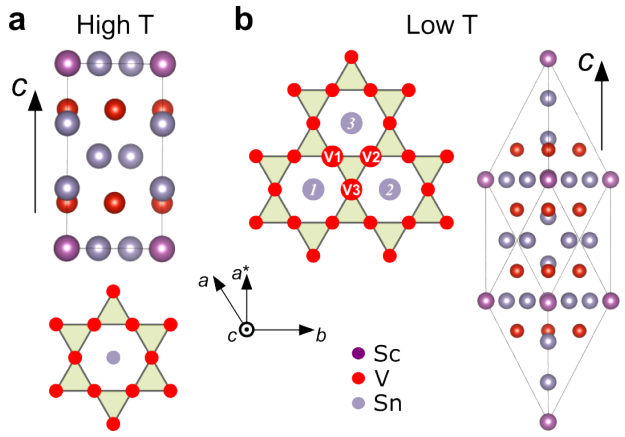

Fig. 1: Crystal structure of ScV_6Sn_6 at (a) high and (b) low temperatures. V atoms (red) form kagome layers. The CDW phase is characterized by an enlarged unit cell dowing to the displacement of Sc and Sn atoms along the c-axis. Adapted from [1].

The kagome metal ScV_6Sn_6 is the only compound in the RV_6Sn_6 family (R = Sc, Y, or a rare earth element) that transforms into a charge-ordered phase at temperatures below 96 K. However, unlike related V-based kagome systems like AV_3Sb_5 (A = K, Rb, or Cs), ScV_6Sn_6 shows no superconductivity at low temperatures and ambient pressure [8, 9]. The CDW phase is unusual in that it affects the position of Sc and Sn atoms along the *c*-axis, while the V kagome plane remains largely unaltered (Figure 1). Still, the states near or at the Fermi level (that is, the electrons contributing to electronic transport, thus being at the center of most sought-after phenomena) belong chiefly to bands with V *d*-orbital character [9]. This bears important consequences for NMR. Before we present the results of the present study, we first introduce the use of NMR to study CDWs.

NMR and Charge Density Waves

NMR is a versatile means of accessing and characterizing the chemical and electronic properties of a material with atomic-scale resolution. It provides a detailed account of local magnetic and electric fields via the interaction between nuclei and their direct surrounding. Typically, fluctuations of the local magnetic field owing to thermally excited electrons, allow also access to the dynamics of a system, which reflect material properties such as characteristic temperature dependencies.

The manifestation of a CDW may be understood as a periodic alteration of the electronic density in real space [10]. In compounds like ScV_6Sn_6, the CDW periodicity coincides with (multiples of) the lattice constant; that is,

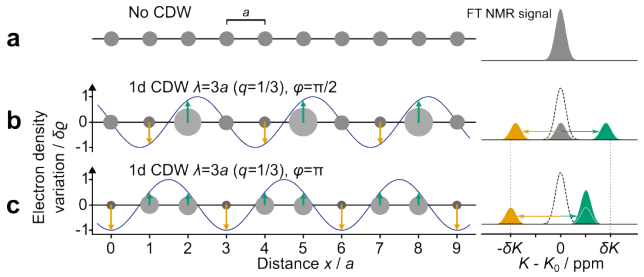

Fig. 2: (a) An atomic chain with evenly distributed electronic density (reflected by the circle sizes) gives a single NMR signal. (b, c) Periodic modulation of the electronic density with a periodicity of 3 results in three resonances, which are characteristically shifted to higher and lower frequencies depending on the relative position of the electronic density wave with respect to the lattice (charge density wave phase φ). Adapted from [1].

the CDW is said to be commensurate. From the perspective of NMR, the changes in the local environments of formerly equivalent nuclei yield characteristic resonance patterns, as exemplified in Figure 2. For commensurate CDW systems with sufficiently short periodicity, the alternating electronic density creates a certain number of local environments, resulting in just as many resonances in the NMR spectrum. Moreover, the resonance pattern enable the locations of the hills and valleys of the wave to be correlated with the crystal sites; that is, it is possible to determine the phase of the corresponding sinusoidal modulation [1, 11]. Hence, NMR is an excellent tool for evaluating the microscopic structure and corresponding electronic properties of CDW systems. In the system of ScV_6Sn_6 current investigations are limited to ^{51}V nuclei, because the Sc and Sn electronic states are located far from the Fermi level, leaving their nuclei almost no means to exchange energy with the environment. Thus Sc and Sn NMR is extremely time consuming.

CDW Phase Transition

The CDW phase transition occurs between 96 and 80 K and appears as a characteristic splittings of the static NMR spectrum. The best way to observe the CDW phase transition, however, is through the corresponding dynamics of the local field. We traced the spin-lattice relaxation time T_1 – characteristic time-scale of the spin system to equilibrium in an external field – from room temperature to 4 K (Figure 3). In metallic systems, spin-lattice relaxation reflects fluctuations due to free carriers and is thus related to the density of states (DOS) [2] as

$$\frac{1}{T_1} \propto (D(E))^2 \,, \qquad (1)$$

where $D(E)$ denotes the DOS as a function of energy E.

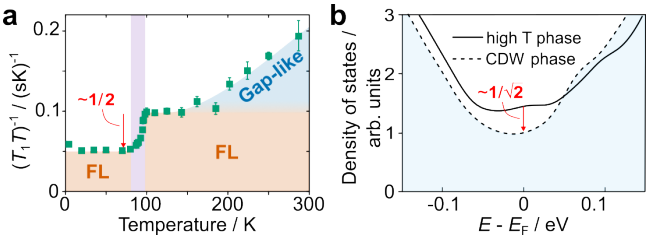

Fig. 3: (a) Spin-lattice relaxation rate as a function of temperature, obtained with the magnetic field parallel to the crystal c-axis. (b) Calculated density of states (DOS) for high- and low-temperature structures. At the Fermi level, the DOS difference of a factor of ~ $\sqrt{2}$ between both phases perfectly fits the relaxation data. Adapted from [1].

A typical consequence of a CDW transition is a loss in DOS. The relaxation data in Figure 3a show the CDW phase transition as a clear drop by a factor of ~ 2 between 96 and 80 K. The calculated DOS in Figure 3b agrees perfectly with the experimental data under the assumption of Eq. (1). Our experimental data further suggest that the low-temperature phase shows Fermi liquid behavior, similarly to the high temperature phase below approximately 150 K. Above that temperature, the upswing of $(T_1T)^{-1}$ is indicative of an increase in DOS due to the separation of the band structure features, such as van Hove singularities by an energy gap. The complexity of the band structure in the present case, however, prevents its exact assignment.

The spin-lattice relaxation rate, as shown in Figure 3a,

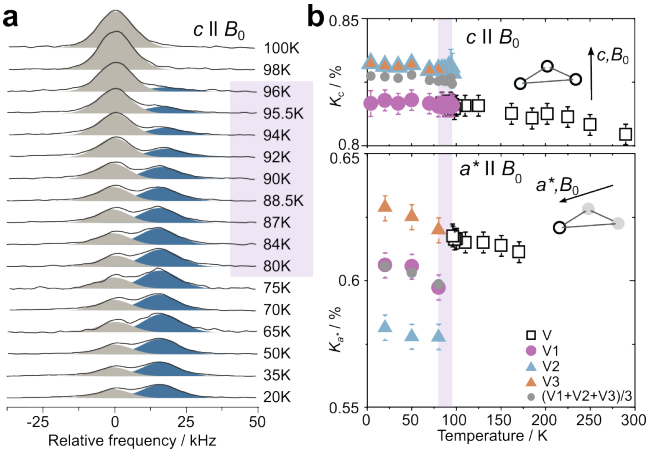

Fig. 4: (a) V spectra for c ∥ B_0 as a function of temperature between 100 and 20 K. During the charge density wave (CDW) phase transition, an additional resonance line appears. (b) V NMR shift data (variation of the local magnetic field) as a function of temperature for c ∥ B_0 and a^* ∥ B_0. During the CDW phase transition, the V resonance splits into three equally intense components (V1, V2, V3) that form different patterns depending on the field orientation. Adapted from [1].

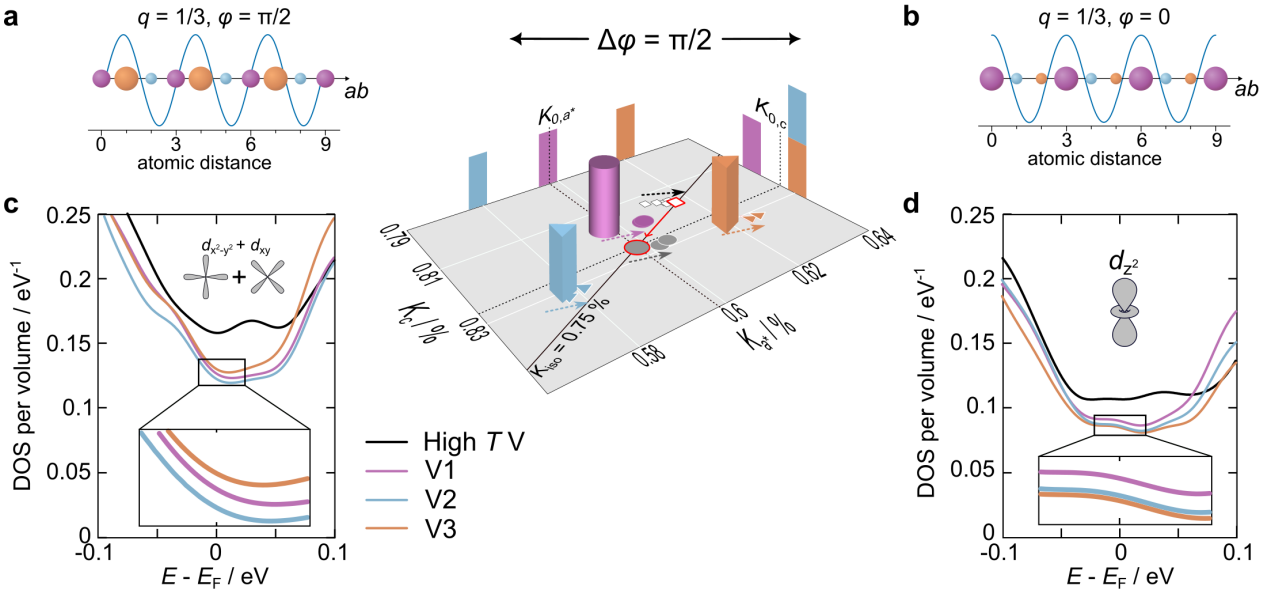

Fig. 5: In the center, the three V components V1, V2, and V3 (3D objects refer to 80 K) and how they are connected to the two different line splittings observed for $c \parallel B_0$ and $a^* \parallel B_0$ (as projections on the K_c and the K_{a^*} axes). The temperature is an implicit parameter. The resonance splittings represent sinusoidal modulations with a periodicity of three but with different phases φ, as shown in panels (a) and (b) (the circle size reflects DOS, whereas the colors denote the three crystal sites). Similar to the corresponding NMR splitting behavior, the site-selective DOS for the in-plane orbitals – panel (c) – reveals a symmetric threefold splitting, whereas the out-of-plane orbital DOS – panel (d) – splits asymmetrically, similar to the NMR signals for $c \parallel B_0$. Adapted from [1].

was measured under an external field along the c-axis (perpendicular to the kagome planes). In the window at which the drop in relaxation was observed, the corresponding static magnetic field changed as well, yielding resonance patterns as described in the former section in Figure 2b and 2c. A detailed account of the V NMR signal during the emergence of the CDW phase for $c \parallel B_0$ is provided in Figure 4. Between 96 and 80 K an additional resonance line (dark blue) appeared next to the initial one (gray). Below 80 K, the asymmetric double-peak remained unchanged. At first glance, it appears rather surprising that the high T resonance appears to survive the CDW phase transition, as this suggests that some fraction of the sample remains in the high T phase. Detailed analysis of the spectral components (including the local charge symmetry [1]) of the NMR signal, however, consistently suggests that the CDW phase doublet consists of *three* individual resonances, each of them different to the high-temperature resonance. That is, as expected from a first-order phase transition, the high T phase is entirely replaced during the CDW phase transition. Three signals is to be expected from the low-temperature crystal structure owing to the presence of three non-equivalent sites, as indicated in Figure 1 by V1, V2, and V3. What is astonishing, though, is that the spectrum – an asymmetric doublet – breaks the threefold symmetry of the structure. This remarkable phenomenon is not readily resolved and demonstrates that the splitting patterns of the local magnetic field in the CDW phase may hold further surprises.

With the magnetic field aligned along the crystal a^*-axis, another threefold splitting is observed; however for this field orientation, the splitting is symmetric. Hence, depending on the magnetic field orientation, the three V components V1 to V3 form different patterns, as shown in Figure 4b. In the language of periodic modulation of the electronic density, as described in Figure 2, the patterns belong to two waves with a phase difference of $\Delta\varphi = \pi/2$ (Figure 2a and 2b).

Orbital and Site Selective Modulation of the DOS

When considering the two mentioned splitting patterns of the NMR signal in the CDW phase, it is important to note that the NMR resonance frequency reflects two components: a spin density (DOS) at the nucleus and a hyperfine interaction. Since the observed splittings are small (150-250 ppm), it is reasonable to assume that the hyperfine interaction, including an anisotropy, is the same for the 3 V sites. Therefore, the different splitting symmetries for the two field orientations must reflect changes in the relative weight of the local electronic spin density; that is, the DOS for each V site apparently changes with the field orientation.

Although tempting to invoke direct interference of the external magnetic field with the modulation of the lo-

cal DOS in terms of a magnetic field-induced phase shift, there is another possible explanation to account for this finding. The two different splittings may reflect two different modulations − substructures in the CDW − while the magnetic field orientation selects between these components via the hyperfine interaction. Hyperfine coupling can be highly anisotropic, because some contributions depend on the geometry of the involved orbitals, as for example in the case of dipolar hyperfine interactions. In other words, the discrepancy of the two different NMR splittings can be resolved by two different DOS modulations for in- and out-of-plane orbitals. The peculiar NMR data and corresponding periodic modulations are summarized in Figure 5. In addition, the orbital-specific DOS, as calculated with DFT, for the three different V sites in the CDW phase are shown on the left and right sides. Consistently, the DOS of the in-plane orbitals $d_{x^2-y^2} + d_{xy}$ (for symmetry reasons, both orbitals are equivalent) splits symmetrically into three components in the CDW phase (Figure 5, bottom left). The DOS of the out-of-plane d_{z^2}-orbital, surprisingly, splits asymmetrically with V2 and V3 having identical low temperature DOS (Figure 5, bottom right). Thus, orbitals and site selective modulations of the DOS in combination with highly anisotropic hyperfine interactions can plausibly explain the observed NMR signal splitting discrepancy.

Summary

The application of ^{51}V NMR to investigate the kagome metal ScV_6Sn_6 has revealed valuable information on its local chemical and electronic structure in the context of a emerging CDW. As expected, the total DOS shrinks as a consequence of CDW formation, as witnessed by the quantitative agreement between the experimental spin-lattice relaxation rate and the results from DFT. The local magnetic field further reveals an unexpected substructure of the low-temperature DOS, not only site, but also orbital dependent, forming individual orbital and site selective modulations of the same periodicity but in different phases.

References

[1]* *Orbital selective commensurate modulations of the local density of states in ScV_6Sn_6 probed by nuclear spins*, R. Guehne, J. Noky, C. Yi, C. Shekhar, M. G. Vergniory, M. Baenitz, and C. Felser, Nat. Commun. **15** (2024) 8213, https://dx.doi.org/10.1038/s41467-024-52456-6

[2] *Emergent Weyl fermion excitations in TaP explored by ^{181}Ta quadrupole resonance*, H. Yasuoka, T. Kubo, Y. Kishimoto, D. Kasinathan, M. Schmidt, B. Yan, Y. Zhang, H. Tou, C. Felser, A. P. Mackenzie, and M. Baenitz, Phys. Rev. Lett. **118** (2017) 236403, https://dx.doi.org/10.1103/PhysRevLett.118.236403

[3]* *Comparative 181Ta-NQR Study of Weyl monopnictides TaAs and TaP: Relevance of Weyl fermion excitations*, T. Kubo, H. Yasuoka, B. Dóra, D. Kasinathan, Y. Prots, H. Rosner, T. Fujii, M. Schmidt, and M. Baenitz, J. Phys. Soc. Jpn. **92** (2023) 094706 https://dx.doi.org/10.7566/JPSJ.92.094706

[4]* *Static and dynamic electronic properties of Weyl semimetal NbP–A single crystal ^{93}Nb-NMR study*, T. Kubo, H. Yasuoka, D. Kasinathan, K. M. Ranjith, M. Schmidt, and M. Baenitz, J. Phys. Soc. Jpn. **93** (2024) 114704 https://doi.org/10.7566/JPSJ.93.114704

[5]* *Experimental nuclear quadrupole resonance and computational study of the structurally refined topological semimetal $TaSb_2$*, T. Fujii, O. Janson, H. Yasuoka, H. Rosner, Y. Prots, U. Burkhardt, M. Schmidt, and M. Baenitz, Phys. Rev. B **109** (2024) 035116, https://dx.doi.org/10.1103/PhysRevB.109.035116

[6] *Magnetic excitations in a topological superconductor, 1T-$MoTe_2$ under pressure*, T. Fujii, H. Yasuoka, M. O. Ajeesh, D. Kashinathan, M. Schmidt, C. Petrovic, and M. Baenitz, (2024), Under progress

[7]* *Fermi surface of the skutterudite* $CoSb_3$*: Quantum oscillations and band-structure calculations*, M. Naumann, P. Mokhtari, Z. Medvecka, F. Arnold, M. Pillaca, S. Flipo, D. Sun, H. Rosner, A. Leithe-Jasper, P. Gille, M. Baenitz, and E. Hassinger, Phys. Rev. B **103** (2021) 085133, https://dx.doi.org/10.1103/PhysRevB.103.085133

[8] *AV_3Sb_5 kagome superconductors*, S. Wilson, and B. Ortiz, Nat. Rev. Mater. **9** (2024) 420–432, https://dx.doi.org/10.1103/RevModPhys.60.1129

[9] *Charge density wave in kagome lattice intermetallic ScV_6Sn_6*, H. W. S. Arachchige, W. R. Meier, M. Marshall, T. Matsuoka, R. Xue, M. A. McGuire, R. P. Hermann, H. Cao, and D. Mandrus, Phys. Rev. Lett. **129** (2022) 216402, https://dx.doi.org/10.1103/PhysRevLett.129.216402

[10] *NMR search for charge density waves*, D. Follstaedt, and C. P. Slichter, Phys. Rev. B **13** (1976) 1017–1027, https://dx.doi.org/10.1103/physrevb.13.1017

[11] *Locally commensurate charge-density wave with three-unit-cell periodicity in $YBa_2Cu_3O_y$*, I. Vinograd, R. Zhou, M. Hirata, T. Wu, H. Mayaffre, S. Krämer, R. Liang, W. N. Hardy, D. A. Bonn, and M.-H. Julien, Nat. Commun. **12** (2021) 3274, http://dx.doi.org/10.1038/s41467-021-23140-w

#robin.guehne@cpfs.mpg.de